Cell Tissue Bank (2022) 23:313–324
https://doi.org/10.1007/s10561-021-09945-5

Improved cell seeding efficiency and cell distribution in porous hydroxyapatite scaffolds by semi-dynamic method

Feng Shi · Ke Duan · Zaijun Yang · Yumei Liu · Jie Weng

Received: 26 February 2021 / Accepted: 28 June 2021 / Published online: 12 July 2021

Abstract Tissue engineering is a promising technique for the repair of bone defects. An efficient and homogeneous distribution of cell seeding into scaffold is a crucial but challenging step in the technique. Murine bone marrow mesenchymal stem cells were seeded into porous hydroxyapatite scaffolds of two morphologies by three methods: static seeding, semi-dynamic seeding, or dynamic perfusion seeding. Seeding efficiency, survival, distribution, and proliferation were quantitatively evaluated. To investigate the performance of the three seeding methods for larger/thicker scaffolds as well as batch seeding of numerous scaffolds, three scaffolds were stacked to form assemblies, and seeding efficiencies and cell distribution were analyzed. The semi-dynamic seeding and static seeding methods produced significantly higher seeding efficiencies, vitalities, and proliferation than did the dynamic perfusion seeding. On the other hand, the semi-dynamic seeding and dynamic perfusion seeding methods resulted in more homogeneous cell distribution than did the static seeding. For stacked scaffold assemblies, the semi-dynamic seeding method also created superior seeding efficiency and longitudinal cell distribution homogeneity. The semi-dynamic seeding method combines the high seeding efficiency of static seeding and satisfactory distribution homogeneity of dynamic seeding while circumventing their disadvantages. It may contribute to improved outcomes of bone tissue engineering.

Keywords Porous scaffold · Cell seeding · Semi-dynamic seeding · Batch samples

F. Shi · Z. Yang · Y. Liu
Collaboration and Innovation Center of Tissue Repair Material Engineering Technology, China West Normal University, Nanchong 637009, Sichuan, China

F. Shi · Z. Yang
College of Life Science, China West Normal University, Nanchong 637009, Sichuan, China

K. Duan
Sichuan Provincial Laboratory of Orthopaedic Engineering, Department of Orthopaedics, The Affiliated Hospital of Southwest Medical University, Luzhou 646000, Sichuan, China

Y. Liu (✉)
College of Environmental Science and Engineering, China West Normal University, Nanchong 637009, Sichuan, China
e-mail: liuyumei@cwnu.edu.cn

J. Weng (✉)
China Key Laboratory of Advanced Technologies of Materials, School of Materials Science and Engineering, Southwest Jiaotong University, Chengdu 610031, Sichuan, China
e-mail: jweng@swjtu.edu.cn

Abbreviations

HA	Hydroxyapatite
3D	Three-dimension
MTT	3-(4, 5-dimethylthiazol-2-yl)-2, 5-diphenyltetrazolium bromide
LDH	Lactate dehydrogenase
MSCs	Mesenchymal stem cells

Introduction

Tissue engineering uses three-dimension (3D) porous scaffolds to support cell proliferation and differentiation into functional tissues for the restoration of human tissues (Ding et al. 2015). In this technique, cell seeding on a scaffold is the first and a crucial step affecting subsequent events, such as cell-scaffold interactions and cellular activities. Homogeneous distribution of cells in a 3D porous scaffold is a desirable starting point for successful tissue engineering, but it remains a technical challenge. As opposed to routine monolayer culture on a flat surface, seeding cells into a porous scaffold is a difficult process, during which the cells need to penetrate into a tortuous structure by migration (Zhang et al. 2015). The distribution of cells seeded into the scaffold is influenced by multiple factors such as cell concentration, incubation time, and the material and microstructure of the scaffold (Costantini et al. 2016; Du et al. 2019). Current methods for cell seeding can be categorized into static and dynamic approaches. In static seeding, a cell suspension is added dropwise onto the scaffold and allowed to infiltrate (under gravity) over time. Although widely used, it frequently involves a low cell seeding efficiency (i.e., percentage of cells remaining inside the scaffold after incubation) and an inhomogeneous cell distribution in the scaffold (Lv et al. 2016; Vitacolonna et al. 2013, 2015). In dynamic seeding, an external force (e.g., vacuum, centrifuge, spinning, perfusion) is used to drive the motion of the cell across the scaffold (Ding et al. 2015; Kleinhans et al. 2015; Melchels et al. 2011). These forces, however, may potentially create mechanical damage to the cells (Melchels et al. 2011; Zhang et al. 2015).

Here, we report an effective semi-dynamic cell seeding method to improve the efficiency and homogeneity of cell seeding. Two types of 3D porous hydroxyapatite ($Ca_{10}(OH)_2(PO_4)_6$, HA) scaffolds with different microstructural characteristics were used for the study (Li et al. 2016a; Shi et al. 2017; Zhao et al. 2009). The objective of this study was to investigate how these different seeding methods (i.e., static seeding, semi-dynamic seeding, and dynamic perfusion seeding) may affect the cell seeding efficiency and the homogeneity, viability, and proliferation of the cells seeded. Furthermore, in an attempt to compare the application of the three seeding methods to larger scaffolds or batch seeding of numerous samples, we characterized the performance of these methods when applied to vertically stacked scaffold assemblies.

Materials and methods

HA scaffold preparation

Two types of 3D porous HA scaffolds were prepared by a porogen-based method and a polymer impregnation method, respectively (Shi et al. 2017; Zhao et al. 2009). In the first method, an HA slurry (20 wt% HA in a 2 wt% sodium alginate solution) was loaded in a cylindrical mold (diameter 20 mm, high 5 cm) prepacked with calcium alginate hydrogel beads (diameter: 1300–1400 μm), and pushed with a plunger to pass though the beads. Then, the mold was immersed in a 0.1 M $CaCl_2$ solution to induce gelation of the HA slurry. The product was dried in air at 40 °C overnight and calcined at 1200 °C for 2 h to form a porous HA scaffold. In following sections, these scaffolds are named Type-I.

In the second method, cylinders (diameter 20 mm, high 2 cm) of polyurethane foam (pore size: ~300 μm; Xinchengfa Filter Equipment, Shenzhen, Guangdong, China) was immersed in an HA slurry (30 wt% HA in a 5 wt% polyvinyl alcohol solution) for five times to form a slurry coating on the struts. Subsequently, the samples were dried at 100 °C overnight, heated at 600 °C for 2 h to burn out the foam, and sintered at 1200 °C for 2 h. These are named Type-II scaffolds. All scaffolds prepared were Φ10 × 8 mm in size.

Mesenchymal stem cell isolation

Mesenchymal stem cells (MSCs) were isolated from Sprague Dawley rats (7–10 days old) as follows (Soleimani and Nadri 2009). The bone marrow in the

intramedullary canals of the tibiae and femurs was flushed out with culture medium and resuspended in low-glucose Dulbecco's modified Eagle medium (LG-DMEM, Gibco, Thermo Fisher, Waltham, MA, USA) supplemented with 100 U/mL penicillin, 100 mg/mL streptomycin, 2 mM L-glutamine, and 10 % fetal bovine serum. The cells were cultured (5 % CO_2, 37 °C) for 1 d; non-adherent cells were discarded; and the medium was renewed. The adherent cells were further cultured and passaged to a 65–70 % confluence.

Seeding methods.

All scaffolds were sterilized by autoclaving (121 °C, 30 min) and rehydrated in LG-DMEM for 2 h at 37 °C. Cells were seeded on scaffolds by three methods as shown in Fig. 1. MSCs were harvested with 0.25 % Trypsin-EDTA solution for 3 min at 37 °C, counted with a hemocytometer and then resuspended to a certain concentration in cell medium. Throughout the study, 5×10^5 cells were seeded on each scaffold, but the cell concentration and the volume of the suspension were varied as described below.

Static seeding

Scaffolds were placed in a 24-well plate; a cell suspension was pipetted on the top of each scaffold in two manners: 50 µL of suspension containing 1×10^7 cells/mL or 100 µL containing 5×10^6 cells/mL (Fig. 1a). The scaffolds were incubated (37 °C, 5 % CO_2, 100 % relative humidity) for 2 h to allow cell attachment and further characterized as described below.

Semi-dynamic seeding

A scaffold was placed in a semi-dynamic seeding system consisting of a silicone tube and a rubber plunger (Fig. 1b). Similarly, 50 µL of the suspension containing 1×10^7 cells/mL or 100 µL containing 5×10^6 cells/mL was pipetted on the scaffold. The plunger was drawn slowly to aspirate the suspension into the scaffold. Then, the scaffolds were incubated for 2 h. During incubation, the plunger was reciprocated three times.

Dynamic perfusion seeding

A custom-made perfusion bioreactor was placed in an incubator (37 °C, 5 % CO_2, 100 % relative humidity). A scaffold was placed in the bioreactor ensuring that LG-DMEM flowed vertically through the scaffold (Fig. 1c). Cell suspension (20 mL of LG-DMEM containing 5×10^5 cells) was loaded into the bioreactor and driven to flow through the scaffold (1 mL/min) with a peristaltic pump. The flow time was set to 2 or 6 h.

Cell seeding efficiency.

Seeding efficiencies for both type-I and type-II scaffolds were determined by measuring the metabolic activities of the cells seeded (Vitacolonna et al. 2015). After the 2-h incubation for cell attachment, 1.5 mL of LG-DMEM was added to each scaffold and incubated

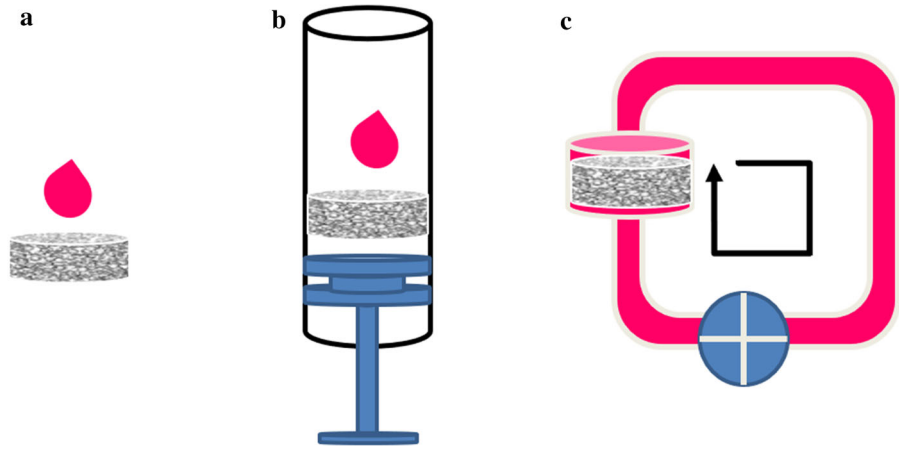

Fig. 1 Schematic illustration of three seeding methods used; **a** static seeding; **b** semi-dynamic seeding; **c** dynamic perfusion seeding. The black arrow indicates the flow direction of the cell suspension

under standard conditions for 12 h. Subsequently, they were transferred to a new 24-well plate, and 2 mL of 3-(4, 5-dimethylthiazol-2-yl)-2,5-diphenyltetrazolium bromide (MTT) reagent (5 mg/mL MTT in LG-DMEM) was added into each well. The reagent was transformed by mitochondrial dehydrogenase into visually dark blue formazan deposits. After incubation at 37 °C for 4 h, the culture medium was discarded, and formazan was solubilized with dimethyl sulfoxide. The absorbance at 490 nm was measured with a microplate reader (Synergie HT, Bio-Tek, Winooski, VT, USA).

Cell membrane integrity, proliferation, distribution, and apoptosis.

Membrane integrity

Damage to cells seeded on type-I scaffolds was evaluated by measuring cell membrane integrity, as indicated by the level of lactate dehydrogenase (LDH) leaked into the culture medium. After incubation for 24 h, the medium was collected and centrifuged (500 *g*, 10 min). The supernatant was assayed with commercial LDH kits (Nanjing Jiancheng Bioengineering Institute, Nanjing, Jiangsu, China) following manufacturer's instructions. LDH release by MSCs seeded in 24-well plates (10^5 cells/well) was measured and served as the control. Cell membrane integrity was expressed as: activity measured from medium/activity from control.

Cell proliferation

After incubation for 1, 3, 5, and 7 d, cell proliferation was assayed by Alamar Blue tests. The scaffold was rinsed with PBS, immersed in fresh culture medium containing 10 % Alamar Blue reagent (Invitrogen, Carlsbad, CA, USA), and incubated at 37 °C for 4 h. Then, 200 μL of the liquid was aspirated to a 96-well plate and the absorbances at 570 and 600 nm were measured. The data were expressed as percentage of Alamar Blue reduction that correlates with the number of cells. LG-DMEM was used as the blank control.

Cell distribution

Confocal laser scanning microscopy was used to characterize cell distribution on the scaffold. After incubation for 7 d, scaffolds were rinsed twice with PBS and incubated (37 °C, in the dark) in PBS containing 5 μM calcein-AM for 30 min. Images were recorded (Nikon A1 plus) from ~ 0 to 1000 μm under the scaffold surface and reconstructed to 3D models (Nikon NIS Viewer 2.5.5) to visualize cell distribution and migration.

Cell apoptosis

After incubation for 5 d, the scaffold was rinsed twice with cold PBS, and the cells were detached by immersion in 2mL of 0.5 % trypsin. The cell suspension was centrifuged at 1000 rpm for 3 min before removed the supernatant. Then added PBS to wash cells, centrifuged at 1000 rpm for 3 min and removed supernatant. They were stained with Annexin V-FITC Apoptosis Detection Kit (Beijing 4 A Biotech, Beijing, China) and analyzed by flow cytometry (FACS ARIA II; BD Biosciences, San Jose, CA, USA). Data were analyzed (FlowJo 7.6.1; Tree Star, Ashland, OR, USA) by quantifying the fluorescence emitted by Annexin V (phosphatidylserine: apoptotic cells) and PI (DNA: dead cells) in each event. A single-cell gate was used to exclude aggregated cells (doublets, triplets), and 30,000 gated events were collected for each analysis. The cells with DNA content less than that of cells at the G1 phase were identified as apoptotic cells.

Seeding on stacked scaffold assembly.

It was envisioned that, larger and thicker scaffolds than those described in previous sections may also be required in clinics. Thus, it would be important to compare the distribution of cells seeded into thicker scaffolds by different methods. Three scaffolds were stacked vertically to form a cylindrical assembly. Each assembly thus formed was seeded by the three methods as if it had been one, albeit thicker, scaffold. In each assembly, the three scaffolds were termed (from top to bottom) layers 1, 2, and 3, respectively. After seeding, the assembly was unassembled, and each scaffold was incubated (37 °C, 5 % CO_2, 100 % relative humidity) for 2 h to allow cell attachment separately. Subsequently, they were analyzed by MTT test (Sec. 4.4.1) to quantitate cells in the three layers.

Statistical analysis

All data were expressed as mean ± standard deviation. The differences between two groups were

analyzed by *t*-test. Differences between three groups were analyzed by analysis of variance (ANOVA; SPSS 15.0, IBM, Armonk, NY, USA) and Tukey multiple comparison test. A p-value < 0.05 was considered statistically significant, and a p-value < 0.01 highly significant.

Results

Scaffold morphology

The type-I scaffold had a cancellous morphology with interconnected spherical macropores (average size: 754 ± 21 μm) (Fig. 2a). The type-II scaffold showed a foam-like morphology with an average macropore size of 275 ± 17 μm (Fig. 2b). The porosities of the two types of scaffolds were 82.5 ± 3.7 % and 87.3 ± 2.9 %, respectively. With satisfactory permeability but highly different pore size ranges, the two types of scaffolds were deliberately used to examine the applicability of the three seeding methods.

Cell seeding efficiency and cell membrane integrity

Identical number (5×10^5) of cells were seeded on all scaffolds under different conditions (suspension volume, cell density, inoculation time) to compare seeding efficiencies and screen optimal parameters. For type-I scaffolds, by static seeding, addition of 50 μL of cell suspension gave a significantly higher seeding efficiency than adding 100 μL ($p < 0.01$) (Fig. 3a). For semi-dynamic seeding, however, no statistically significant difference was observed between addition of 50 μL or 100 μL. For dynamic perfusion seeding, perfusion for 6 h yielded a significantly higher seeding efficiency than did perfusion for 2 h ($p < 0.01$). Furthermore, comparison of the three seeding methods working under their optimal conditions found that, static seeding and semi-dynamic seeding produced significantly higher seeding efficiencies than dynamic seeding ($p < 0.01$) (Fig. 3a).

Similar trend and statistical differences in seeding efficiency were also observed from Type-II scaffolds (Fig. 3b). Comparison between the two types of scaffolds found that, under comparable conditions (e.g., suspension volume, inoculation time), seeding efficiencies were slightly higher in the Type-II than in Type-I. This may be explained by the smaller pore size and larger specific surface area of the Type-I, which offers a greater area for cell adhesion.

The LDH level in the medium indicates the degree of cell membrane damage caused by the cell seeding operation. For type-I scaffolds, the LDH levels measured after static seeding and semi-static seeding were 4.53 % ($p = 0.0029$) and 4.38 % ($p = 0.0093$) lower than that recorded after dynamic seeding (Fig. 3c), respectively; both differences were highly statistically significant. Additionally, the LDH level measured after semi-static seeding was 0.15 % ($p = 0.237$) lower than that from static seeding, and the difference was not statistically significant. These indicate that, the repeated aspiration force generated by the semi-dynamic seeding method was mild so that the damage was markedly reduced (vs. dynamic

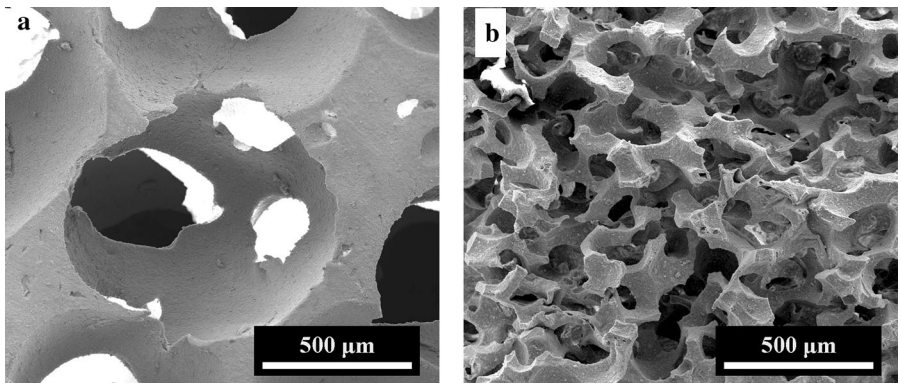

Fig. 2 Scanning electron micrographs of **a** type-I and **b** type-II scaffolds

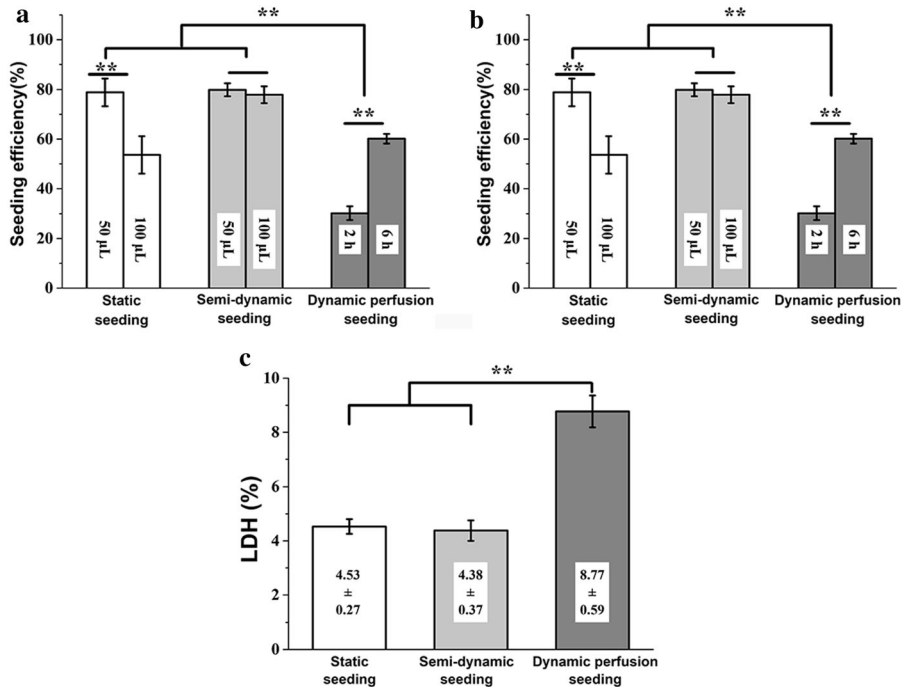

Fig. 3 Cell seeding efficiencies of three seeding methods for **a** type-I and **b** type-II scaffolds and **c** LDH levels measured from cells seeded

perfusion seeding). Similar trends were observed from type-II scaffolds (not shown for brevity).

Cell proliferation, distribution, and apoptosis

Figure 4a depicts the proliferating profiles of the cells seeded on type-I scaffolds. Generally, cells seeded by all three methods proliferated well, exhibiting classical tri-phasic curves. At the first phase (1–3 d), the cell proliferation was negligible (for dynamic seeding) to moderate (for static and semi-static seeding). On day 1, the scaffolds seeded by the dynamic method contained 13.0 % fewer cells than those seeded by the static method, as may be expected from its lower seeding efficiency (Fig. 3). At the second phase (3–5 d), the cell numbers increased by 15.0 % (static seeding), 24.6 % (semi-static seeding), and 12.9 % (dynamic seeding), respectively. At the third phase (5–7 d), the cell number further increased (vs. day 5) by 1.88 % (static seeding), 12.1 % (semi-static seeding), and 5.41 % (dynamic seeding), respectively.

Fluorescence microscopy of type-I scaffolds seeded by the static method revealed a large number of cells and a substantial cell aggregation (Fig. 4b). In comparison, the scaffolds seeded by the semi-dynamic method gave a more homogeneous cell distribution (Fig. 4c). This appears to be consistent with the greater proliferation between days 3–7 of cells seeded by the semi-dynamic method compared with those seeded by the static one (Fig. 4a), as homogeneously distributed cells would experience less contact inhibition. The scaffolds seeded by the dynamic method showed a small number of cells but a uniform distribution (Fig. 4d), as may be expected from its lowest seeding efficiency and dynamic nature.

Flow cytometry revealed that, after incubation for 5 d, the proportions of apoptotic cells seeded on the type-I scaffolds by the semi-dynamic method or the dynamic method were both significantly lower than that derived from the static method (both $p < 0.01$) (Fig. 4e-g). Furthermore, the proportion of apoptosis cells (Q2 + Q3) measured from the semi-dynamic method was 2.64 % lower than that from the dynamic one, and the difference was not statistically significant ($p = 0.183$). These show that the semi-dynamic and dynamic seeding methods yielded similar cell viabilities. Similar trends in cell proliferation, distribution,

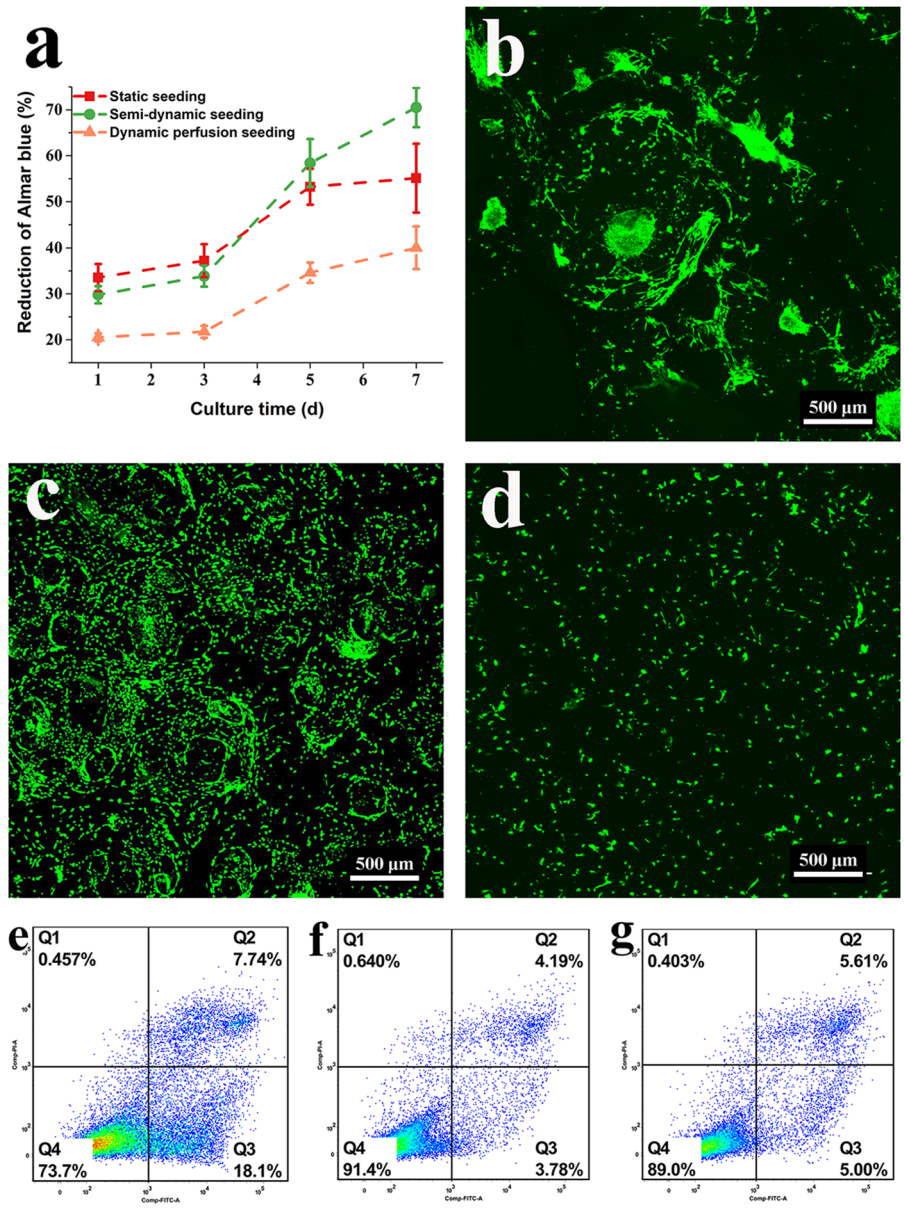

Fig. 4 Proliferation curves, fluorescence micrographs and apoptosis of cells seeded on type-I scaffolds by (**b**, **e**) static seeding, (**c**, **f**) semi-dynamic seeding, and (**d**, **g**) dynamic perfusion seeding. (**e**-**g**) Flow cytometry plots: Q1 represents necrotic cells; Q2 represents cells at a late stage of apoptosis; Q3 represents cells at a late stage of apoptosis, Q4 represents viable cells

and apoptosis were also observed from type-II scaffolds (not shown).

Seeding into scaffold assembly.

To compare the performance of different seeding methods for larger scaffolds, three scaffolds were vertically stacked, and seeding efficiency and cell distribution for such stacked assemblies were investigated. Generally, for both types I and II scaffolds, the overall seeding efficiencies (i.e., averaged seeding efficiencies for layers 1–3) measured from scaffold assemblies were similar to those recorded from individual scaffolds (Fig. 5 vs. 2). Furthermore, compared with dynamic perfusion

seeding, the static and semi-dynamic seeding methods yielded higher overall seeding efficiencies (Fig. 5).

Type-I scaffolds

After static seeding, 51.7 % of the seeded cells were distributed in layer 2 whereas layer 1 retained 20.7 % (Fig. 5a). This pattern appears because the large pores of the scaffolds allow easy downflow of the cell suspension under gravity, preventing layer 1 from fully retaining the suspension. Additionally, the suspension is held in the pores by interfacial forces such as capillary force; consequently, when the suspension moves to certain depth, the area of interaction becomes sufficiently large to hold the suspension (vs. gravity). This discourages further downward flow of the suspension, resulting a low seeding efficiency at layer 3.

After semi-dynamic seeding, 32.6 %, 34.3 %, and 33.1 % of the cells were distributed in layers 1–3 (Fig. 5a), and ANOVA found no statistically significant difference among the three layers, indicating the homogenizing effect of the aspiration movement of the plunger. After dynamic perfusion seeding, 35.3 %, 31.8 %, and 32.9 % of the cells were distributed in layers 1–3, exhibiting a homogeneity expected from the continuous flow of the suspension.

Type-II scaffolds

Compared with the type-I scaffolds, the type-II showed generally similar trends of seeding efficiencies but slightly higher values (Fig. 5b). This marginal difference is probably attributable to the smaller pores of the type-II, which provided a larger surface area for cell adhesion. Additionally, after static seeding, layer 1 had a significantly higher seeding efficiency than layers 2 and 3 (79.05 % vs. 16.68 % and 4.27 %). This is also explained by the small pores of the type-II, which impedes the initial downward flow of the suspension. In comparison, after semi-dynamic or dynamic perfusion seeding, the three layers had homogeneous distribution of cells.

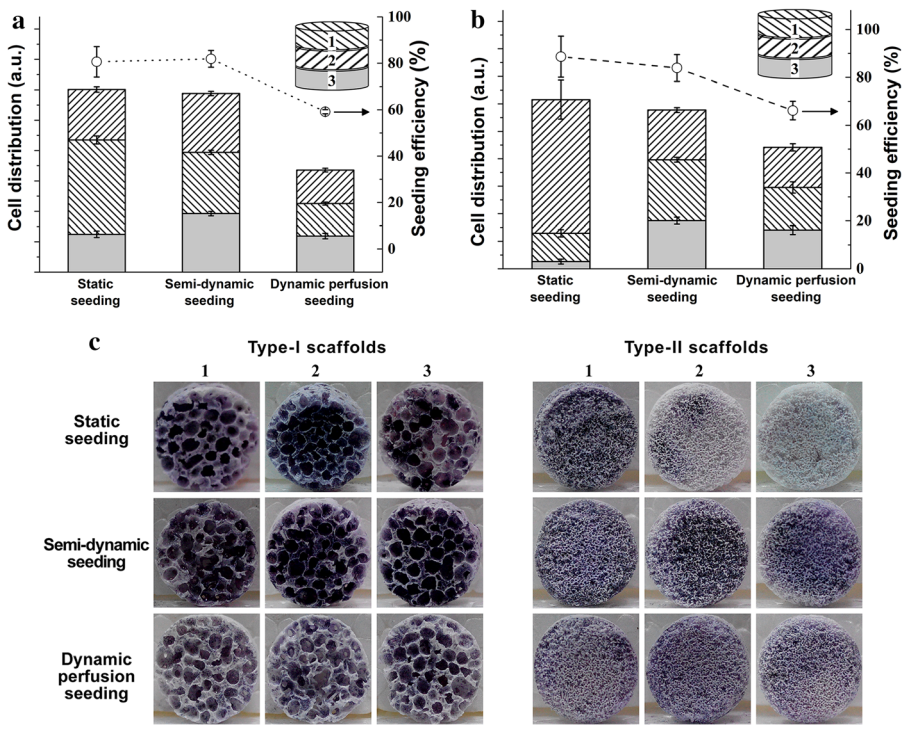

Fig. 5 Layer-wise cell seeding efficiencies for **a** type-I and **b** type-II scaffolds and **c** cell distribution in three layers of scaffold assemblies

MTT staining

MTT staining of each layer showed that, for both types of scaffolds, after semi-dynamic seeding or dynamic perfusion seeding, the three layers were relatively homogeneously stained (Fig. 5c). Those seeded by the dynamic perfusion were more lightly stained compared with those seeded by the semi-dynamic method, consistent with its lower seeding efficiencies (Fig. 5a-b). Moreover, after static seeding, the type-I assembly exhibited a more intense staining in layer 2 than the other layers, and the type-II showed a more intense staining in layer 1, also consistent with above results. These observations demonstrate that, the static seeding is prone to producing longitudinally inhomogeneous cell distribution for relatively thick scaffolds. In comparison, the semi-dynamic and dynamic perfusion seeding offer improved longitudinal homogeneity, with the former giving a higher overall seeding efficiency (Fig. 3).

Discussion

Earlier studies have demonstrated that the distribution of cells on scaffolds affects their subsequent proliferation and differentiation (Hori et al. 2016; McBeath et al. 2004; Theodoridis et al. 2020; Wu et al. 2020). For cells of low proliferating activities or scarce sources, increasing the seeding efficiency is of particular values. A high cell seeding efficiency is conducive to cell-cell communication and signal transmission, thereby promoting the secretion and differentiation of extracellular matrix (McBeath et al. 2004). Hori et al. found that, increasing the efficiency of cell seeding on β-tricalcium phosphate granules contributed to improved *in vivo* bone formation. Therefore, seeding is key to ensuring successful preparation of tissue-engineered constructs (Florczyk et al. 2012; Hori et al. 2016; Salita et al. 2016; Wang et al. 2014; Zhang et al. 2015). Obviously, scaffold microstructure affects the distribution of cells seeded, with a high porosity and permeability benefiting a homogeneous distribution (Chen et al. 2017; Melchels et al. 2010; Olivares and Lacroix 2012).

The conventional static seeding is influenced by factors such as material properties and shape of the scaffold, and it is difficult to ensure the homogeneity and reproducibility of seeding. When the cell suspension is seeded on the surface of a scaffold, it is drawn into the scaffold by gravity and capillary force (Baba Ismail et al. 2018; Bai et al. 2015). When the volume of the cell suspension becomes sufficiently large, the suspension may flow out from the bottom of the scaffold to the well plate, resulting in a significant reduction in the cell seeding efficiency. However, it is impossible to simply minimize the volume of the suspension, as this would impair the homogeneity of cell distribution in the scaffold. Excessively high local cell concentrations (Fig. 5b) also cause injurious effects such as contact inhibition and cell death due to local hypoxia (Dong et al. 2002; Hong et al. 2014). Several strategies have been reported to improve the distribution of cells seeded by static seeding, such as multi-point seeding (Zhang et al. 2015), increasing the viscosity of cell suspension (Cámara-Torres et al. 2020; Choi et al. 2017; Florczyk et al. 2012), and the use of siphoning (Yamanaka et al. 2015). However, due to the passive nature of cell dispersion, static seeding experiences inherent limitations for 3D porous or complex-shaped scaffolds. Jian Dong et al.(Dong et al. 2002) used static seeding method to inoculate bone marrow pre-osteoblasts on a porous β-TCP scaffold and implanted in animals to promote bone formation *in vivo*. However, the new bone tissue was mainly distributed in the periphery of the scaffold, while the internal pores were free of new bone tissue. Combined with the previous analysis of cell inoculation results, it may be due to that the distribution of cells was not uniform after static inoculation, and there were many cells on the surface of scaffolds. With cell proliferation, a layer of cell shielding layer was formed on the surface, which hindered the migration and growth of cells/tissues to the internal pores of scaffolds.

Dynamic seeding methods, especially dynamic perfusion seeding, overcomes the above disadvantages but their seeding efficiencies are generally low (Costantini et al. 2016; Lemonnier et al. 2014), as a result of the use of a large volume of suspension to allow perfusion. Furthermore, at higher flow rates, cells could be detached from the scaffold surface (Kitagawa et al. 2006). In contrast, in our semi-dynamic seeding method, a small volume of suspension was sucked into the scaffold by aspiration, eliminating the disadvantages of both static and dynamic-perfusion seeding methods. This translated into improved seeding efficiency and initial cell

distribution in scaffolds, which favored subsequent proliferation (Figs. 3a−b and 4a).

Cell membrane damage has been frequently overlooked in previous studies of tissue engineering. It impairs normal cell-cell interactions required for tissue engineering and even leads to cell death (Li et al. 2016b). In dynamic-perfusion seeding, cell viability is affected by the flow rate of the suspension (Vila et al. 2016; Zhao and Ma 2005). The fluid flow impairs cell adhesion due to its shearing action (Vila et al. 2016; Zhao and Ma 2005). It can also mechanically damage the cell membrane, leading to LDH release (Yang et al. 2016). Cell membrane damage may further affect cell adhesion, lowering the seeding efficiency. In the semi-dynamic seeding, the aspiration actions were slow and limited to four cycles (i.e., 1 for seeding, 3 during incubation) to minimize potential mechanical damage to the cell membrane. Cell membrane damage may further affect cell adhesion, lowering the seeding efficiency.

Tissue engineering frequently requires biological evaluation of a large number of samples. Ensuring consistency and uniformity during cell seeding is vital. So far, few studies have considered the performance of seeding methods for scaffolds of different microstructures or simultaneous seeding of numerous scaffolds. In the present study, scaffold of two different porous morphologies and stacked scaffold assemblies were evaluated using three seeding methods. Fluorescence microscopy can visualize cell distribution in porous scaffolds, only cells on/near the surface can be observed and the field of view is small (Tuin et al. 2016; Zhang et al. 2015). Histological sectioning can also reveal the distribution of cells in 3D porous scaffolds, but the process is tedious (Ding et al. 2008; Filipowska et al. 2016; Melchiorri et al. 2016). In this study, stacking of multiple scaffold layers combined with MTT staining (Reinwald et al. 2014; Su et al. 2014) provided a straightforward technique for characterizing the longitudinal distribution of viable cells in the scaffold. This technique showed that, consistent with previous assay results (Fig. 5a−b), scaffolds seeded by the three methods had different numbers and patterns of viable cell distribution cells (Fig. 5c) with the semi-dynamic one producing the optimal homogeneity and seeding efficiency.

Conclusions

A semi-dynamic seeding method was developed for seeding MSCs on 3D porous HA scaffolds. This method produced an increased seeding efficiency and decreased cell membrane damage compared with dynamic perfusion seeding method. It also yielded an improved initial cell distribution homogeneity compared with the common static seeding method. Thus, this method integrates the advantages of the other two methods while circumventing their disadvantages. This new method is expected to launch a new application in bone tissue engineering.

Acknowledgements This research was funded by National Natural Science Foundation of China (2016YFB0700803), Sichuan Science and Technology Program (2020065, 21MZGC0218), Major Project of Education Department in Sichuan Province (18CZ0019), Startup Program of Southwest Normal University (18Q069, 18Q030), Luzhou-SWMU Strategic Cooperation Program (2017LZXNYD-J35).

Funding No competing financial interests exist.

Data Availability Statements The datasets generated during and analyzed during the current study are available from the corresponding author on reasonable request.

Declarations

Conflict of interest The authors declare no conflict of interest.

References

Baba Ismail YM, Reinwald Y, Wimpenny I, Bretcanu O, Dalgarno K, El Haj AJ (2018) The Influence of Scaffold Designs on Cell Seeding Efficiency in Establishing A Three-Dimensional Culture Journal of Physics: Conference Series 1082:012072 doi:https://doi.org/10.1088/1742-6596/1082/1/012072

Bai H, Wang D, Delattre B, Gao W, De Coninck J, Li S, Tomsia AP (2015) Biomimetic gradient scaffold from ice-templating for self-seeding of cells with capillary effect. Acta Biomat 20:113–119. doi:https://doi.org/10.1016/j.actbio.2015.04.007

Cámara-Torres M, Sinha R, Mota C, Moroni L (2020) Improving cell distribution on 3D additive manufactured scaffolds through engineered seeding media density and viscosity. Acta Biomat 101:183–195. doi:https://doi.org/10.1016/j.actbio.2019.11.020

Chen GB, Xu R, Zhang C, Lv YG (2017) Responses of MSCs to 3D scaffold matrix mechanical properties under oscillatory perfusion. Culture Acs Appl Mater Interf 9:1207–1218. doi:https://doi.org/10.1021/acsami.6b10745

Choi WI, Yameen B, Vilos C, Sahu A, Jo S-M, Sung D, Tae G (2017) Optimization of fibrin gelation for enhanced cell seeding and proliferation in regenerative medicine applications Polymers. Adv Technol 28:124–129. doi:https://doi.org/10.1002/pat.3866

Costantini M et al (2016) Correlation between porous texture and cell seeding efficiency of gas foaming and microfluidic foaming scaffolds. Mater Sci Eng: C 62:668–677. doi:https://doi.org/10.1016/j.msec.2016.02.010

Ding C-M, Zhou Y, He Y-N, Tan W-S (2008) Perfusion seeding of collagen–chitosan sponges for dermal tissue engineering. Process Biochem 43:287–296. doi:https://doi.org/10.1016/j.procbio.2007.12.005

Ding M, Henriksen SS, Wendt D, Overgaard S (2015) An automated perfusion bioreactor for the streamlined production of engineered osteogenic grafts. J Biomed Mater Res Part B Appl Biomater 104:532–537. doi:https://doi.org/10.1002/jbm.b.33407

Dong J, Uemura T, Shirasaki Y, Tateishi T (2002) Promotion of bone formation using highly pure porous β-TCP combined with bone marrow-derived osteoprogenitor. Cells Biomater 23:4493–4502. doi:https://doi.org/10.1016/S0142-9612(02)00193-X

Du Y, Guo JL, Wang J, Mikos AG, Zhang S (2019) Hierarchically designed bone scaffolds: From internal cues to. External Stimuli Biomater 218:119334. doi:https://doi.org/10.1016/j.biomaterials.2019.119334

Filipowska J, Reilly GC, Osyczka AM (2016) A single short session of media perfusion induces osteogenesis in hBMSCs cultured in porous scaffolds. Dependent Cell Differ Stage Biotechnol Bioeng 113:1814–1824. doi:https://doi.org/10.1002/bit.25937

Florczyk SJ et al (2012) Enhanced bone tissue formation by alginate gel-assisted cell seeding in porous ceramic scaffolds and sustained release of growth factor. J Biomed Mater Res Part A 100A:3408–3415. doi:https://doi.org/10.1002/jbm.a.34288

Hong M-H, Kim S-M, Om J-Y, Kwon N, Lee Y-K (2014) Seeding cells on calcium phosphate scaffolds using hydrogel enhanced osteoblast proliferation and differentiation. Ann Biomed Eng 42:1424–1435. doi:https://doi.org/10.1007/s10439-013-0926-z

Hori A, Agata H, Takaoka M, Tojo A, Kagami H (2016) Effect of cell seeding conditions on the efficiency of vivo bone formation. Int J Oral Maxillofac Implants 31:232–239. doi:https://doi.org/10.11607/jomi.4729

Kitagawa T, Yamaoka T, Iwase R, Murakami A (2006) Three-dimensional cell seeding and growth in radial-flow perfusion bioreactor for in vitro tissue reconstruction. Biotechnol Bioeng 93:947–954. doi:https://doi.org/10.1002/bit.20797

Kleinhans C et al (2015) A perfusion bioreactor system efficiently generates cell-loaded bone substitute materials for addressing critical size bone defects. Biotechnol J 10:1727–1738. doi:https://doi.org/10.1002/biot.201400813

Lemonnier S et al (2014) Dynamic mesenchymal stem cells volumic seeding in a commercialized porous ceramic scaffold: a feasibility study. Comput Methods Biomech BioMed Eng 17:4–5. doi:https://doi.org/10.1080/10255842.2014.931049

Li J et al (2016a) Ectopic osteogenesis and angiogenesis regulated by porous architecture of hydroxyapatite scaffolds with similar interconnecting structure in vivo. Regen Biomater 3:285–297. doi:https://doi.org/10.1093/rb/rbw031

Li Y, Wang J, Xing J, Wang Y, Luo Y (2016b) Surface chemistry regulates the sensitivity and tolerability of osteoblasts to various magnitudes of fluid shear stress. J Biomed Mater Res Part A 104:2978–2991. doi:https://doi.org/10.1002/jbm.a.35848

Lv XG et al (2016) Comparative study of different seeding methods based on a multilayer SIS scaffold: Which is the optimal procedure for urethral tissue engineering? J Biomed Mater Res Part B: Appl Biomater 104:1098–1108. doi:https://doi.org/10.1002/jbm.b.33460

McBeath R, Pirone DM, Nelson CM, Bhadriraju K, Chen CS (2004) Cell shape, cytoskeletal tension, and RhoA regulate stem cell lineage commitment. Developmental cell 6:483–495. doi:https://doi.org/10.1016/s1534-5807(04)00075-9

Melchels FPW, Barradas AMC, van Blitterswijk CA, de Boer J, Feijen J, Grijpma DW (2010) Effects of the architecture of tissue engineering scaffolds on cell seeding and culturing. Acta Biomater 6:4208–4217. doi:https://doi.org/10.1016/j.actbio.2010.06.012

Melchels FPW et al (2011) The influence of the scaffold design on the distribution of adhering cells after perfusion cell seeding. Biomaterials 32:2878–2884. doi:https://doi.org/10.1016/j.biomaterials.2011.01.023

Melchiorri AJ, Bracaglia LG, Kimerer LK, Hibino N, Fisher JP (2016) In vitro endothelialization of biodegradable vascular grafts via endothelial progenitor cell seeding and maturation in a tubular perfusion system bioreactor tissue engineering Part C. Methods 22:663–670. doi:https://doi.org/10.1089/ten.tec.2015.0562

Olivares AL, Lacroix D (2012) Simulation of cell seeding within a three-dimensional porous scaffold: a fluid-particle analysis tissue engineering part. C-Methods 18:624–631. doi:https://doi.org/10.1089/ten.tec.2011.0660

Reinwald Y, Johal RK, Ghaemmaghami AM, Rose FRAJ, Howdle SM, Shakesheff KM (2014) Interconnectivity and permeability of supercritical fluid-foamed scaffolds and the effect of their structural properties on cell distribution. Polymer 55:435–444. doi:https://doi.org/10.1016/j.polymer.2013.09.041

Salita S, Amornsudthiwat P, Damrongsakkul S, Kanokpanont S (2016) An axial distribution of seeding, proliferation, and osteogenic differentiation of MC3T3-E1 cells and rat bone marrow-derived mesenchymal stem cells across a 3D Thai silk fibroin/gelatin/hydroxyapatite scaffold in a perfusion bioreactor. Mater Sci Eng: C: C 58:960–970. doi:https://doi.org/10.1016/j.msec.2015.09.034

Shi F, Zhi W, Liu Y, Zhou T, Weng J (2017) One-step method to construct hydroxyapatite scaffolds with 3-D interconnected structure by a novel hydrogel bead porogen process. Mater Lett 203:13–16. doi:https://doi.org/10.1016/j.matlet.2017.05.099

Soleimani M, Nadri S (2009) A protocol for isolation and culture of mesenchymal stem cells from mouse bone marrow. Nat Protoc 4:102–106. doi:https://doi.org/10.1038/nprot.2008.221

Su W-T, Wang Y-T, Chou C-M (2014) Optimal fluid flow enhanced mineralization of MG-63 cells in porous chitosan scaffold. J Taiwan Inst Chem Eng 45:1111–1118. doi:https://doi.org/10.1016/j.jtice.2013.10.016

Theodoridis K et al (2020) An effective device and method for enhanced cell growth in 3D scaffolds: Investigation of cell seeding and proliferation under static and dynamic conditions. Mater Sci Eng: C 114:111060. doi:https://doi.org/10.1016/j.msec.2020.111060

Tuin SA, Pourdeyhimi B, Loboa EG (2016) Fabrication of novel high surface area mushroom gilled fibers and their effects on human adipose derived stem cells under pulsatile fluid flow for tissue engineering applications. Acta Biomater 36:220–230. doi:https://doi.org/10.1016/j.actbio.2016.03.025

Vila OF et al (2016) Real-time bioluminescence imaging of cell distribution, growth, and differentiation in a three-dimensional scaffold under interstitial perfusion for tissue engineering tissue engineering part C. Methods 22:864–872. doi:https://doi.org/10.1089/ten.tec.2014.0421

Vitacolonna M, Belharazem D, Hohenberger P, Roessner ED (2013) Effect of static seeding methods on the distribution of fibroblasts within human acellular dermis. Biomed Eng Online 12:55. doi:https://doi.org/10.1186/1475-925X-12-55

Vitacolonna M, Belharazem D, Hohenberger P, Roessner ED (2015) Effect of dynamic seeding methods on the distribution of fibroblasts within human acellular dermis. Cell Tissue Banking 16:605–614. doi:https://doi.org/10.1007/s10561-015-9508-7

Wang L et al (2014) Repair of segmental bone defect using totally vitalized tissue engineered bone graft by a combined perfusion seeding and culture. System Plos One 9:e94276. doi:https://doi.org/10.1371/journal.pone.0094276

Wu YF, Chen C, Tang JB, Mao WF (2020) Growth and stem cell characteristics of tendon-derived cells with different initial seeding densities: an in vitro study in mouse flexor tendon cells. Stem Cells Dev 29:1016–1025. doi:https://doi.org/10.1089/scd.2020.0036

Yamanaka K et al (2015) Seeding of mesenchymal stem cells into inner part of interconnected porous biodegradable scaffold by a new method with a filter paper. Dent Mater J 34:78–85. doi:https://doi.org/10.4012/dmj.2013-330

Yang Y et al (2016) Melatonin reverses flow shear stress-induced injury in bone marrow mesenchymal stem cells via activation of AMP-activated protein kinase signaling. J Pineal Res 60:228–241. doi:https://doi.org/10.1111/jpi.12306

Zhang Z-Z, Jiang D, Wang S-J, Qi Y-S, Zhang J-Y, Yu J-K (2015) Potential of centrifugal seeding method in improving cells distribution and proliferation on demineralized cancellous bone scaffolds for tissue-engineered meniscus. ACS Appl Mater Interfaces 7:15294–15302. doi:https://doi.org/10.1021/acsami.5b03129

Zhao F, Ma T (2005) Perfusion bioreactor system for human mesenchymal stem cell tissue engineering: dynamic cell seeding and construct development. Biotechnol Bioeng 91:482–493. doi:https://doi.org/10.1002/bit.20532

Zhao J, Lu X, Duan K, Guo L, Zhou S, Weng J (2009) Improving mechanical and biological properties of macroporous HA scaffolds through composite coatings. Colloids Surf B 74:159–166. doi:https://doi.org/10.1016/j.colsurfb.2009.07.012